Supporting information

Impact of initial surface roughness and aging on coke formation during Ethane Steam Cracking

Stamatis A. Sarris[1], Steffen H. Symoens[1], Natalia Olahova[1], Kim Verbeken[2], Marie-Françoise Reyniers[1], Guy B. Marin[1], Kevin M. Van Geem[1,*]

[1]Ghent University, Laboratory for Chemical Technology, Technologiepark 914, 9052 Gent, Belgium.

[2]Ghent University, Department of Materials Science and Engineering, Technologiepark 903, 9052 Gent, Belgium

[*]Corresponding author: Technologiepark 914, 9052 Gent, Belgium; Kevin.VanGeem@UGent.be

Supporting information

Coke formation mechanisms

The carbon deposition process during thermal cracking in the presence, or not, of steam, is a quite complex phenomenon. It has been extensively described in literature[1-4] that it mainly consists of three mechanisms; catalytic coke formation, coke growth from existing carbon layers onwards and gas phase coking, as illustrated in Figure S. 1.

The initial phase of carbon deposition is the formation of a porous network of carbon filaments, catalyzed typically by Ni and Fe present at the surface of the reactor walls. It is widely accepted that catalytic carbon formation[5-9] on metallic surfaces involves surface reactions, diffusion and precipitation of carbon. As a first step, a hydrocarbon molecule is chemisorbed on a metal crystallite of the surface. Dehydrogenation of the R-CH groups takes place with the hydrogen atoms recombining and desorb into the gas phase. As a result, the carbon atoms are formed at the surface, dissolve in and diffuse through the metal particle. The carbon accumulation in the particle causes a pressure build up at the dislocations and the grain boundaries, which may exceed the tensile strength of the metal.

Potentially, the metal particle is then lifted from the surface and carbon crystallizes at the rear end of the particle. Growing stems are developed that carry crystallites on their top. The precipitation of the carbon can give rise to structural deficiencies in the carbon lattice, thereby creating reactive carbon sites along this layer. Additional hydrocarbon molecules from the gas phase are incorporated at these sites causing addable filamentous coke growth. In that way, a porous layer of interwoven filaments is developed. The metal particles at the top of the whiskers are becoming more accessible from the gas phase. Therefore the deposition rate increases, while the diffusion rate through the metal remains stable. Carbon migration over the metal surface occurs, surrounding the carbon stems. At this point, surface carbon can occur, encapsulating the metal and terminating any further coke growth.

Dissociative chemisorption of water molecules on the metal particles produces highly reactive oxygen atoms that react with surface carbon to from carbon monoxide, which desorbs in the gas phase. This reaction prevents the fast encapsulation of the metal tip of the filament and therefore the termination of this reaction, in other words the "deactivation of the metallic active site". How quickly these phenomena are occurring is a matter of relative kinetics of carbon growth, gasification, dissolution and diffusion. Certainly, the properties of the alloy are very important in all the mechanisms, however in this study the composition was kept stable to isolate the effect of roughness.

The heterogeneous non-catalytic mechanism is the major source of coke in an industrial cracker, since it takes place over the complete run length. The coke in contact with the gas phase looks like a succession of several discrete layers, deriving from the coke-gas interface[10, 11]. Coke formation is described by the reaction of gas phase precursors with active centers of the surface. Kopinke et al[1] have provided a general scale for the coking tendency of several precursors. For example, acetylene, anthracenes, cyclic naphthenes and aromatics possess a high tendency for coke formation. Ethylene is not the most reactive one, however due to its high concentration is very important. No significant differences of the relative constants of a particular hydrocarbon were found for different materials[1], supporting that the active centers are radical in nature and positioned in the coke matrix. The radicals can be generated by hydrogen abstraction from the partially dehydrogenated carbon layer being determined by the gas phase composition and the available coked reactor surface[12]. The coke radicals

react by addition with unsaturated molecules and radicals from the gas phase. After dehydrogenation, graphitic layers are formed[13].

The last mechanism, also known as homogeneous non-catalytic coking results from a sequence of molecular and/or radical reactions in the gas phase. These lead to high molecular weight polynuclear aromatic compounds which remain solid even at high temperatures. As a result, they collide at the wall and integrate in the coke layer[14]. In this work, the latter mechanism contributes very little, since there are not a lot heavy compounds generated in the gas phase due the light feedstock (ethane).

Jet stirred reactor

A small coupon of dimensions 10 mm x 8 mm x 1 mm is hanged by the arm of the electro balance in the center of a spherical jet stirred reactor, right above the jets, as illustrated in Figure S. 2. As recently published by our research group and is represented in Figure S. 3 [15], the mixing is quite ideal, with negligible changes of the gas phase concentrations and temperature around the coupon. Therefore, the set-up is suitable for the study of coke formation on high temperature alloys.

Coking rates

The coking rates presented in this paper, see Table S. 2, have been calculated using the geometric surface of the samples. In order to calculate the coking rates based on the real sample surface, parameters such as the sampling length of the equipment used and the mean spacing (S) of the local peaks measured – see Figure S. 4 - should be recorded. The equipment used, a SJ210 Mutitoyo Surface Roughness Tester, does not provide logging of the above mentioned values that would allow the calculation of the real surface of the samples tested. A general idea of the arithmetical range of the mean spacing per surface roughness values, which is summarized in **Error! Reference source not found.** can be given by the operational manual of the equipment[16]. The mean spacing S, for n number of spaces is calculated by the following formula (1):

$$S = \frac{1}{n} \sum_{1}^{n} S_i \qquad (1)$$

From Table S. 3, the S_{min} corresponds to the minimum theoretically expected mean spacing, while the S_{max} is representative of the maximum value of the theoretically expected mean spacing for the measured R_α roughness value in each case. The theoretical range of the mean spacing increases by increasing surface roughness.

SEM & EDX results

The analyzed samples are covered by a carbon layer of a different thickness for the different roughness values. However, clearly, based on the penetration depth calculated for carbon, see Table 3 of the manuscript**Error! Reference source not found.**, the EDX data at 10 KV for the coked samples obtained for an initial surface roughness up to 1.3 μm can be expected to be more or less representative of the coupon's oxidized surface. For a higher initial surface roughness it is more appropriate to consider the EDX data at 20 KV. Therefore, it is theoretically possible to extract fruitful observations based on these results. Regarding the impact of the different base metal composition for the different surface roughness values, this is typically the expected result from the EDX analysis.

As compared to the not coked only pre-oxidized sample, the EDX data at 10 kV show that up to an initial surface roughness of 1.3 μm, there is an important increase in the Cr content and a slight increase in the Fe content followed by an pronounced decrease in the Mn content and a slight decrease in Ni content. At 20 kV, the EDX data indicate that for an initial surface roughness of 2.6 μm onwards, the Cr content steadily decreases, the Fe content slightly increases while the Mn content increases and the Ni content remains fairly stable. The amounts of metallic Ni and Fe show a tendency to slightly increase with increasing surface roughness. As both metallic Fe and Ni are well-known catalysts for coke formation, their increased presence at the surface further explain the observed effects on the coking in the catalytic stage[13].

Carbon and Oxygen are excluded by the analysis since their detection is not quantitative by means of EDX. The results obtained are normalized and not "absolute" values, however they

are representative of the oxidized layer existing under the coked surface. For lighter elements, such as Carbon and Oxygen, other techniques could be used.

However, no differences are expected on the elemental composition of the coke layer, since no differences are observed experimentally in terms of asymptotic coking, while the coke structure remains rather stable for all the different surface roughness values. The latter are confirmed by Table S. 2 and Figure 10. As a result, no additional analysis is suggested regarding the Carbon and Oxygen content.

Catalytic coking fraction in steam cracking

Analogously to the studied cracker or set-up, different observations regarding the fraction of the initial coke deposited on the tube surface versus the coke formed during the asymptotic period can be made. Typically in the models describing the coking behavior of industrial crackers presented in the literature[13, 17, 18], only the contribution of heterogeneous non-catalytic coke formation is taken into account. Homogeneous non-catalytic coking only contributes significantly at temperatures higher than $1170\ K$ or during the cracking of heavy feedstocks, e.g. atmospheric gas oil or vacuum gas oil. In order to justify neglecting the catalytic mechanism, the following theory is developed based on observations on coke deposits formed during industrial operation as shown in the work of Reyniers [19].

Based on literature data [20], the average height of the catalytic coking layer in an industrial cracker tube is determined. Combined with the average density of catalytic coke, the amount of catalytic coke deposited on the cracker tube is determined.

$$m_{coke} = h_{coke}\ \rho_{coke} = 100\ 10^{-6}\ [m] * 1.6\ 10^3\ \left[\frac{kg}{m^3}\right] = 0.160\ \left[\frac{kg}{m^2}\right] \tag{2}$$

Based on that, an average coking rate is determined by interpolating exponentially between the maximum coking rate and asymptotic coking rate obtained by experiments in a micro-reactor setup. This average catalytic coking rate is determined to be $2.083\ 10^{-6}\ \frac{kg}{m^2\ s}$ at

$1083\ K$. Combined with an activation energy of $167.36\ 10^3\ \frac{J}{mol}$, a rate expression for catalytic coke formation is determined.

$$r_{coke,av}(catalytic) = 2.45\ 10^2\ \exp\left(-\frac{167.36\ 10^3}{R\ T}\right)\left[\frac{kg}{m^2\ s}\right] \tag{3}$$

Based on these calculations, Reyniers [19] concludes that for temperatures higher than $1070\ K$, the catalytic coking mechanism is only important for about $10\ hrs$ which is in the order of magnitude of $1\ \%$ of the total run length of an industrial cracker. The error made by not considering the catalytic coking mechanism is limited to less than $3\ \%$ which was deemed acceptable by the author.

In the presented work, it is clear that the time needed to reach the asymptotic coking depends on the initial surface roughness. However, overall the asymptotic coking is reached after the first 2-3 hours. Judging by the previous work done in coke formation during steam cracking[13, 17, 21-24], definitely the most important step for the simulation of the run length of an industrial cracker is the representation and prediction of the asymptotic coking, where no significant differences are observed for the – quite broad- studied roughness range.

However, to fundamentally model coke formation the study of all the parameters has equivalent importance. An industrial run length can last from 30 to 150 days[25], depending on the applied process conditions, feedstock and reactor material and geometry. Industrially the initial coking is not expected to be more than the 5 % of the total coke formed on the reactor walls, therefore the roughness will not have a significant effect on the overall run length but it will certainly affect the initial coking behavior of a cracker.
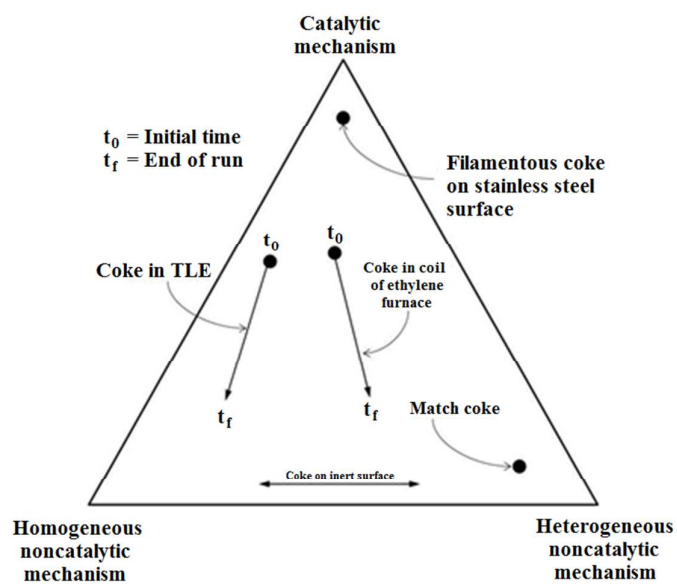
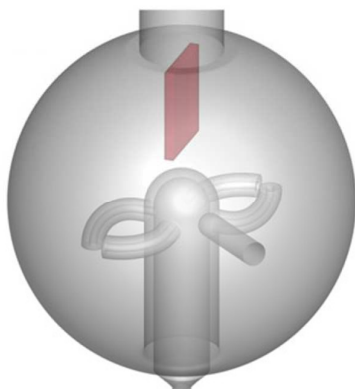Figure S. 1. Comparison of the relative importance of the three main coking mechanisms[26]

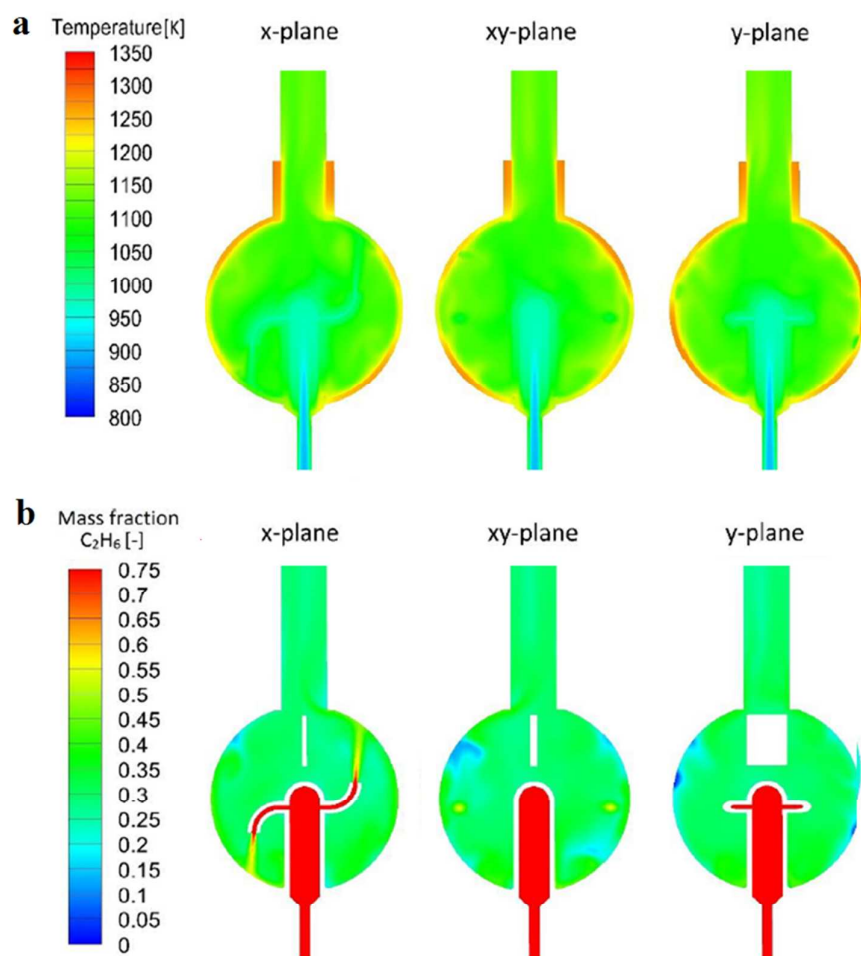Figure S. 2. Coupon position in the reactor

Figure S. 3. Cross section fields of temperature (a) and ethane mass fraction (b) for ethane cracking experiments in the JSR[15]
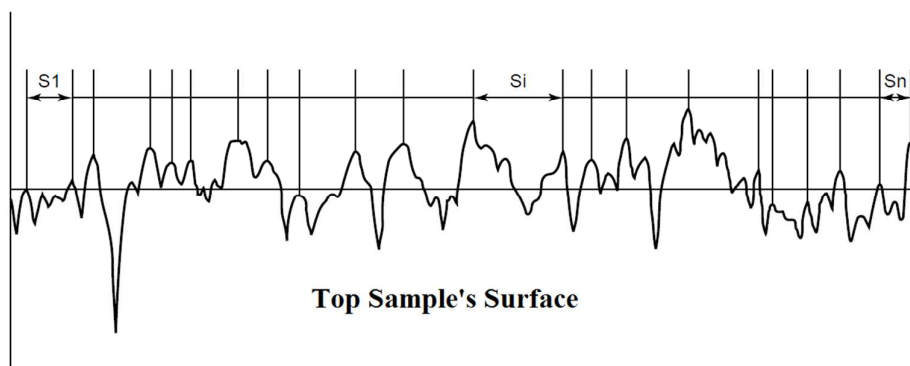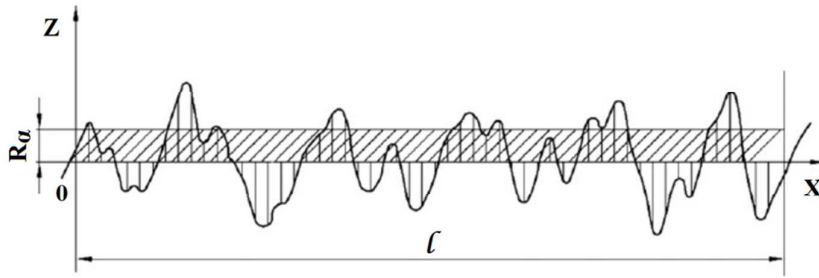

Figure S. 4. Local peaks spacing (Si)[16]

Figure S. 5. Illustration of the determination of the surface roughness. Shown is the height profile of the surface measured over a distance ℓ on the surface with $Z(0)$, the mean value of the measured height profile. R_α, the arithmetic average of the absolute deviations of $Z(x)$ from $Z(0)$, is also indicated.
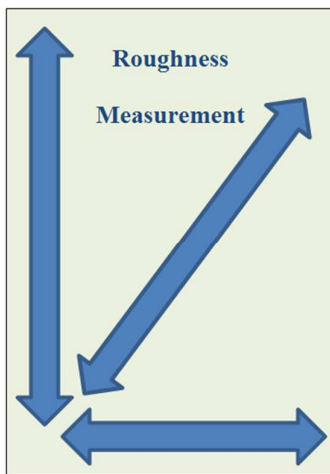

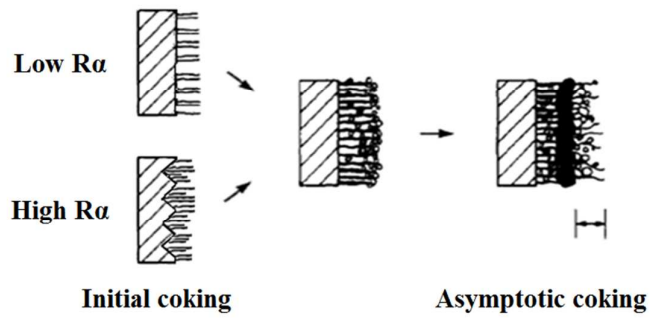Figure S. 6. Illustration of the procedure used to measure the roughness of the tested coupons.

Figure S. 7. Graphical illustration of the limited effect of the initial surface roughness on the asymptotic coking behavior [3]
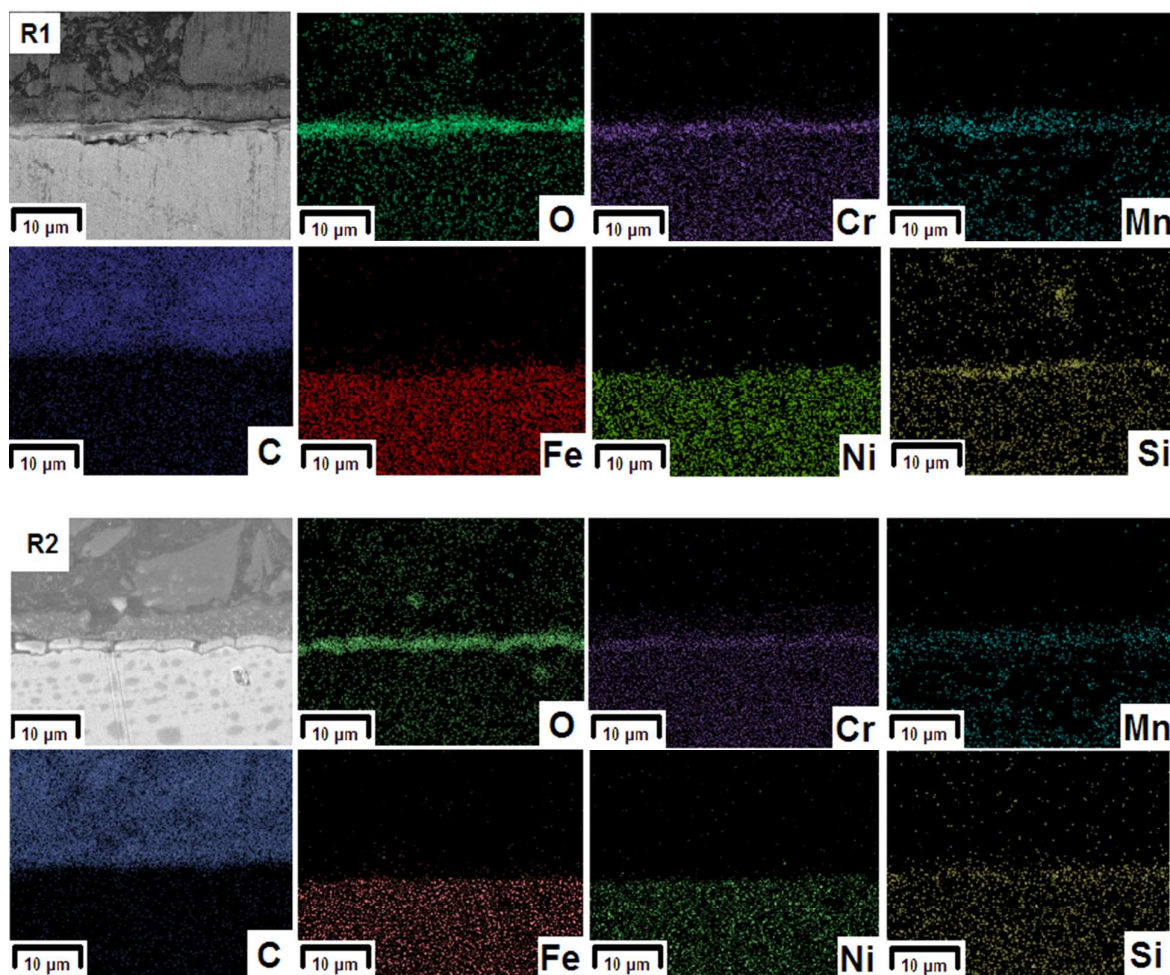
Figure S. 8. Elemental mappings of the coked samples obtained after 1 hour of cracking in the 8th cracking cycle for an initial surface roughness of R1 (0.15 μm), R2 (0.75 μm), R3 (1.3 μm) and R4 (2.6 μm). Magnification: 3000x; Accelerating Voltage: 15 kV; Steam cracking of Ethane: F_{HC} = 29.18 10^{-6} kg s^{-1}, δ = 0.33 kg_{H2O} kg^{-1}_{HC}, $T_{reactor}$ = 1173 K, P = 101.35 kPa, F_{H2O} = 9.72 10^{-6} kg s^{-1}, 8 cracking cycles
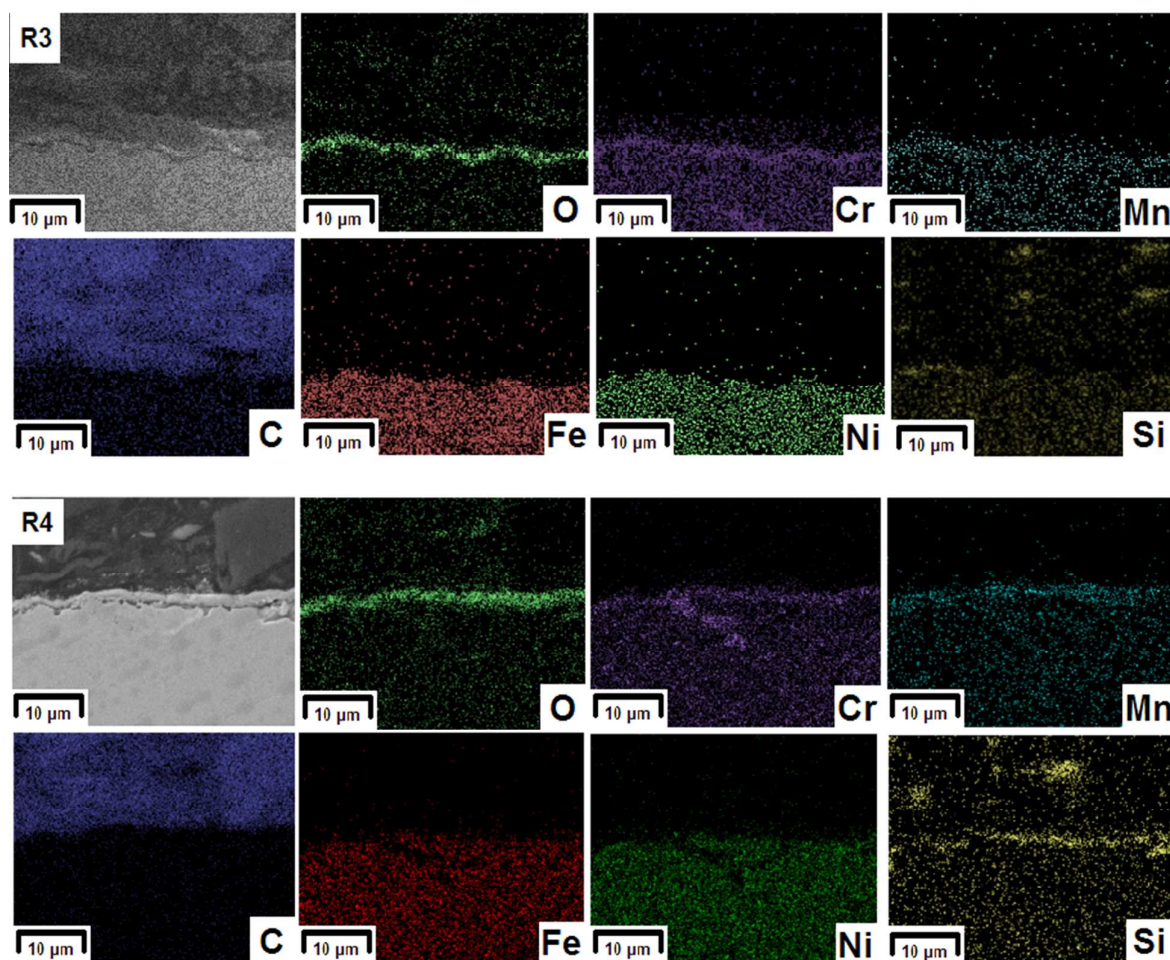
Figure S. 9. Elemental mappings of the coked samples obtained after 1 hour of cracking in the 8th cracking cycle for an initial surface roughness of R1 (0.15 μm), R2 (0.75 μm), R3 (1.3 μm) and R4 (2.6 μm). Magnification: 3000x; Accelerating Voltage: 15 kV; Steam cracking of Ethane: F_{HC} = 29.18 10^{-6} kg s^{-1}, δ = 0.33 kg$_{H2O}$ kg$^{-1}_{HC}$, $T_{reactor}$ = 1173 K, P = 101.35 kPa, F_{H2O} = 9.72 10^{-6} kg s^{-1}, 8 cracking cycles
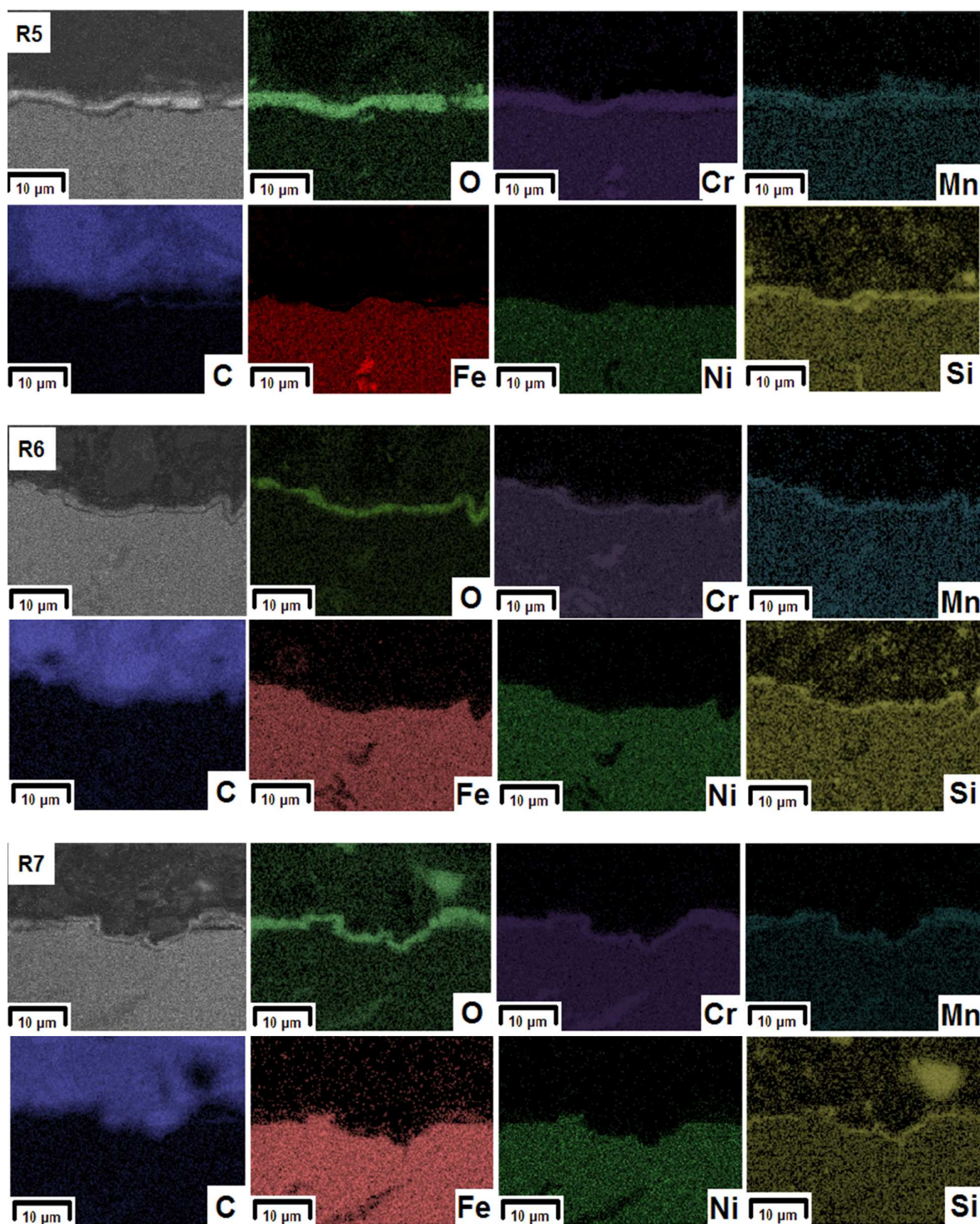
Figure S. 10. Elemental mappings of the coked samples for an initial surface roughness of R5 (3.9 μm), R6 (5.1 μm) and R7 (7.0 μm). Magnification: 3000x; Accelerating Voltage: 15 kV; Steam cracking of Ethane: $F_{HC} = 29.18 \ 10^{-6} \ kg \ s^{-1}$, $\delta = 0.33 \ kg_{H2O} \ kg^{-1}_{HC}$, $T_{reactor} = 1173 \ K$, $P = 101.35 \ kPa$, $F_{H2O} = 9.72 \ 10^{-6} \ kg \ s^{-1}$, 8 cracking cycles

Table S. 1. Overview of the cyclic aging experimental procedure

Process step	Duration	Temperature (K)	Gas feed flow (10^{-6} kg s^{-1})			Water flow (10^6 kg s^{-1})
			N$_2$	Ethane	Air	
Preoxidation	12-14 hours	1023	-	-	9.575	-
High-Temperature Preoxidation	30-40 minutes	Heating up from 1023 to 1173	9.683	-	11.862	-
Steam treatment	15 minutes	1173	-	-	11.862	6.7
1st cc	6 hours	1173	-	29.167	-	9.7
Decoking	30-40 minutes	Heating up from 1023 to 1173	9.683	-	11.862	-
Steam treatment	15 minutes	1173	-	-	11.862	6.7
2nd cc	6 hours	1173	-	29.167	-	9.7
Decoking	30-40 minutes	Heating up from 1023 to 1173	9.683	-	11.862	-
Steam treatment	15 minutes	1173	-	-	11.862	6.7
3rd cc	6 hours	1173	-	29.167	-	9.7
Decoking	30-40 minutes	Heating up from 1023 to 1173	9.683	-	11.862	-
Steam treatment	15 minutes	1173	-	-	11.862	6.7
Cyclic aging	Consists of 4 cycles of: ○ Heating up from 1023 to 1173 K ○ Cracking at 1173 K (1 hour) ○ Decoking from 1023 to 1173 K ○ Steam treatment at 1173 K (15 minutes)					
8th cc	6 hours	1173	-	29.167	-	9.7
Decoking	30-40 minutes	Heating up from 1023 to 1173	9.683	-	11.862	-
Steam treatment	15 minutes	1173	-	-	11.862	6.7
Cooling down	100 K /h	To ambient temperature under He	-	-	-	-

During stabilization points a stable helium flow of 0.14 10^{-6} kg s^{-1} is fed

Table S. 2. Process Conditions, Coking rates and Product Yields of Roughness Study; Steam cracking of Ethane: $F_{HC} = 29.18 \ 10^{-6}$ kg s^{-1}, $\delta = 0.33$ kg$_{H2O}$ kg$^{-1}_{HC}$, $T_{reactor} = 1173$ K, $P = 101.35$ kPa, $F_{H2O} = 9.72 \ 10^{-6}$ kg s^{-1}, 8 cracking cycles

Experiment	R1	R2	R3	R4	R5	R6	R7
R_a Roughness[a] (μm)	0.15±0.02	0.75±0.15	1.3±0.2	2.6±0.2	3.9±0.3	5.1±0.3	7.0±0.4
CC[b]				Mass of coke [10^{-6} kg]			
1	1.1±0.1	1.3±0.1	1.2±0.1	1.2±0.1	1.4±0.1	1.4±0.1	1.6±0.2
2	1.2±0.1	1.2±0.1	1.2±0.1	1.2±0.1	1.5±0.2	1.6±0.2	1.7±0.2
3	1.2±0.1	1.2±0.1	1.4±0.1	1.4±0.1	1.6±0.2	1.8±0.2	1.8±0.2
4	0.5±0.1	0.5±0.1	0.6±0.1	0.7±0.1	0.8±0.1	1.5±0.2	2.3±0.2
5	0.6±0.1	0.6±0.1	0.7±0.1	0.9±0.1	1.4±0.1	1.4±0.1	1.9±0.2
6	0.5±0.1	0.6±0.1	0.7±0.1	0.8±0.1	1.6±0.2	2.6±0.3	2.9±0.3
7	0.4±0.1	0.5±0.1	0.5±0.1	0.8±0.1	1.4±0.1	2.1±0.2	2.8±0.3
8	1.17±0.1	1.2±0.1	1.2±0.1	1.6±0.2	2.0±0.2	3.0±0.3	3.2±0.3
CC				$r_{initial}$ [10^{-7} kg s^{-1} m^{-2}]			
1	3.8±0.4	6.8±0.7	7.0±0.7	6.1±0.6	7.8±0.8	8.9±0.9	12.1±1.2
2	5.8±0.6	6.7±0.7	6.7±0.7	6.1±0.6	9.8±1.0	9.8±1.0	13.8±1.4
3	6.8±0.7	6.9±0.7	8.3±0.9	9.5±1.0	11.4±1.1	14.4±1.4	14.3±1.4
4	7.1±0.7	7.5±0.8	8.2±0.9	9.4±1.0	11.1±1.1	21.1±2.1	32.8±3.3
5	7.9±0.8	8.5±0.9	9.3±1.0	13.2±1.3	19.8±2.0	19.8±2.0	26.2±2.6
6	7.0±0.7	8.4±0.8	9.7±1.0	11.2±1.1	22.4±2.2	37.4±3.7	41.7±4.2
7	6.0±0.6	6.5±0.7	6.7±0.7	11.2±1.1	19.4±2.0	29.2±2.9	39.4±3.9
8	5.8±0.6	6.2±0.6	6.3±0.7	12.1±1.2	17.3±1.7	31.3±3.1	34.4±3.4
CC				$r_{asymptotic}$ [10^{-7} kg s^{-1} m^{-2}]			
1	2.2±0.2	2.3±0.2	2.2±0.2	2.2±0.2	2.3±0.2	2.3±0.2	2.1±0.2
2	2.2±0.2	2.1±0.2	2.2±0.2	2.1±0.2	2.3±0.2	2.5±0.3	2.2±0.2
3	2.1±0.2	2.1±0.2	2.3±0.2	2.1±0.2	2.2±0.2	2.3±0.2	2.3±0.2
8	2.2±0.2	2.2±0.2	2.1±0.2	2.1±0.2	2.2±0.2	2.2±0.2	2.3±0.2
Components				Averaged product Yields over 8 CC [wt % dry]			
H_2	4.2±0.1	4.29±0.1	4.28±0.05	4.29±0.1	4.26±0.1	4.28±0.1	4.31±0.1
CO	0.06±0.01	0.07±0.01	0.08±0.01	0.08±0.01	0.09±0.01	0.09±0.01	0.09±0.01
CO_2	0.002±0.001	0.002±0.001	0.002±0.001	0.002±0.001	0.002±0.001	0.003±0.001	0.003±0.001
CH_4	7.0±0.1	7.3±0.2	7.1±0.2	7.2±0.2	7.1±0.1	7.1±0.1	7.2±0.2
C_2H_6	30.2±0.5	29.5±0.6	29.9±0.5	29.9±0.5	30.0±0.5	29.9±0.5	29.6±0.5
C_2H_4	49.9±0.3	50.2±0.3	49.8±0.3	50.1±0.3	50.1±0.3	50.1±0.2	50.1±0.2
C_3H_8	0.1±0.02	0.12±0.02	0.11±0.02	0.12±0.02	0.12±0.02	0.11±0.02	0.11±0.02
C_3H_6	0.74±0.02	0.74±0.02	0.75±0.02	0.75±0.02	0.75±0.02	0.74±0.02	0.74±0.02
C_2H_2	1.43±0.04	1.44±0.05	1.43±0.05	1.44±0.05	1.43±0.05	1.44±0.05	1.44±0.05
1,3-C_4H_6	1.9±0.1	2.0±0.1	2.0±0.1	2.0±0.1	2.0±0.1	2.0±0.1	2.0±0.1
benzene	2.5±0.1	2.6±0.1	2.5±0.1	2.6±0.1	2.6±0.1	2.5±0.1	2.6±0.1

[a] roughness before pretreatment, [b] cracking cycle

Table S. 3. Theoretical range of the arithmetic range of the mean spacing per surface roughness.[16]

R_α µm [10^{-3} mm]	Smin [10^{-3} mm]	Smax [10^{-3} mm]
0.15	0.0013	0.04
0.75	0.04	0.13
1.3	0.13	0.4
2.6	0.4	1.3
3.9	0.4	1.3
5.1	0.4	1.3
7	0.4	1.3

References

1.   Kopinke, F. D.; Zimmermann, G.; Nowak, S., On the mechanism of coke formation in steam cracking—conclusions from results obtained by tracer experiments. *Carbon* **1988,** 26, (2), 117-124.
2.   Cai, H.; Krzywicki, A.; Oballa, M. C., Coke formation in steam crackers for ethylene production. *Chemical Engineering and Processing: Process Intensification* **2002,** 41, (3), 199-214.
3. Albright, L. F.; Marek, J. C., Mechanistic model for formation of coke in pyrolysis units producing ethylene. *Ind. Eng. Chem. Res.* **1988,** 27, (5), 755-759.
4.   Lahaye, J.; Badie, P.; Ducret, J., Mechanism of carbon formation during steamcracking of hydrocarbons. *Carbon* **1977,** 15, (2), 87-93.
5. Baker, R. T. K.; Yates, D. J. C.; Dumesic, J. A., Filamentous Carbon Formation over Iron Surfaces. In *Coke Formation on Metal Surfaces*, AMERICAN CHEMICAL SOCIETY: 1983; Vol. 202, pp 1-21.
6.Lyle, F. A.; Baker, R. T. K., *Coke Formation on Metal Surfaces*. AMERICAN CHEMICAL SOCIETY: 1983; Vol. 202, p 332.
7.Figueiredo, J. L., Reactivity of coke deposited on metal surfaces. *Materials and Corrosion* **1999,** 50, (12), 696-699.
8.   Snoeck, J.-W.; Froment, G.; Fowles, M., Filamentous carbon formation and gasification: thermodynamics, driving force, nucleation, and steady-state growth. *Journal of Catalysis* **1997,** 169, (1), 240-249.
9. Bonnet, F.; Ropital, F.; Berthier, Y.; Marcus, P., Filamentous carbon formation caused by catalytic metal particles from iron oxide. *Materials and Corrosion* **2003,** 54, (11), 870-880.
10.   Ranzi, E.; Dente, M.; Goldaniga, A.; Bozzano, G.; Faravelli, T., Lumping procedures in detailed kinetic modeling of gasification, pyrolysis, partial oxidation and combustion of hydrocarbon mixtures. *Progress in Energy and Combustion Science* **2001,** 27, (1), 99-139.
11.Kopinke, F. D.; Zimmermann, G.; Reyniers, G. C.; Froment, G. F., Relative rates of coke formation from hydrocarbons in steam cracking of naphtha. 2. Paraffins, naphthenes, mono-, di-, and cycloolefins, and acetylenes. *Ind. Eng. Chem. Res.* **1993,** 32, (1), 56-61.
12.   Wauters, S.; Marin, G. B., Computer generation of a network of elementary steps for coke formation during the thermal cracking of hydrocarbons. *Chemical Engineering Journal* **2001,** 82, (1–3), 267-279.
13.Reyniers, G. C.; Froment, G. F.; Kopinke, F.-D.; Zimmermann, G., Coke Formation in the Thermal Cracking of Hydrocarbons. 4. Modeling of Coke Formation in Naphtha Cracking. *Ind. Eng. Chem. Res.* **1994,** 33, (11), 2584-2590.
14.Bach, G.; Zimmermann, G.; Kopinke, F.-D.; Barendregt, S.; van den Oosterkamp, P.; Woerde, H., Transfer-Line Heat Exchanger Fouling during Pyrolysis of Hydrocarbons. 1. Deposits from Dry Cracked Gases. *Industrial & Engineering Chemistry Research* **1995,** 34, (4), 1132-1139.
15.Reyniers, P. A.; Sarris, S. A.; Marin, G. B.; Van Geem, K. M., Computational Fluid Dynamic Design of Jet Stirred Reactors for Measuring Intrinsic Kinetics of Gas-Phase and Gas-Solid Reactions. *International Journal of Chemical Kinetics* **2016,** 48, (9), 556-569.
16.ltd, B. r. t., MITUTOYO SURFTEST SJ201P - Surface roughness tester Manual. In *178*, www.brw.ch, 2008.
17.Plehiers, P. M.; Reyniers, G. C.; Froment, G. F., Simulation of the run length of an ethane cracking furnace. *Ind. Eng. Chem. Res.* **1990,** 29, (4), 636-641.
18.   Geem, K. M. V.; Dhuyvetter, I.; Prokopiev, S.; Reyniers, M.-F.; Viennet, D.; Marin, G. B., Coke Formation in the Transfer Line Exchanger during Steam Cracking of Hydrocarbons. *Ind. Eng. Chem. Res.* **2009,** 48, (23), 10343-10358.
19. Reyniers, G. C. Cokesvorming bij de Thermische Kraking van Koolwaterstoffen. Rijksuniversiteit Gent, 1992.
20.Bennett, M. J.; Price, J. B., Oxidation of an Ethylene Steam Cracker Pyrolysis Tube Deposit in Water Vapor and Its Enhancement by Inorganic Catalysts. In *Coke Formation on Metal Surfaces*, American Chemical Society: 1983; Vol. 202, pp 59-87.

21.   Van Geem, K. M.; Reyniers, M. F.; Pyl, S. P.; Marin, G. B., Effect of Operating Conditions and Feedstock Composition on Run Length of Steam Cracking Coils. In *(2009) AIChE 2009 Spring National Meeting*, Tampa, FL, 2009.

22. Schietekat, C. M.; Sarris, S. A.; Reyniers, P. A.; Kool, L. B.; Peng, W.; Lucas, P.; Van Geem, K. M.; Marin, G. B., Catalytic Coating for Reduced Coke Formation in Steam Cracking Reactors. *Ind. Eng. Chem. Res.* **2015,** 54, (39), 9525-9535.

23.Muñoz Gandarillas, A. E.; Van Geem, K. M.; Reyniers, M.-F.; Marin, G. B., Influence of the Reactor Material Composition on Coke Formation during Ethane Steam Cracking. *Ind. Eng. Chem. Res.* **2014,** 53, (15), 6358-6371.

24. Muñoz Gandarillas, A. E.; Van Geem, K. M.; Reyniers, M.-F.; Marin, G. B., Coking Resistance of Specialized Coil Materials during Steam Cracking of Sulfur-Free Naphtha. *Ind. Eng. Chem. Res.* **2014,** 53, (35), 13644-13655.

25.Mahamulkar, S.; Yin, K.; Agrawal, P. K.; Davis, R. J.; Jones, C. W.; Malek, A.; Shibata, H., Formation and Oxidation/Gasification of Carbonaceous Deposits: A Review. *Ind. Eng. Chem. Res.* **2016**.

26.Albright, L. F.; Marek, J. C., Mechanistic Model for Formation of Coke in Pyrolysis Units Producing Ethylene. *Ind. Eng. Chem. Res.* **1988,** 27, (5), 755.